Journal of Imaging Science and Technology® 66(2): 020410-1–020410-7, 2022.

Dimensionality Reduction of Spectral Reflectance by Dividing the Error Space of Principal Component Analysis

Junfeng Li and Miaoxin Li
Henan University of Animal Husbandry and Economy, Zhengzhou, 450046, China

Qian Cao
Shanghai Publishing and Printing College, Shanghai, 200093, China

Shiwei Liu and Chun'ao Wei
Henan University of Animal Husbandry and Economy, Zhengzhou, 450046, China
E-mail: 81898@hnuahe.edu.cn

Abstract. *A method based on the error space division of principal component analysis (PCA) is proposed to improve both the spectral and colorimetric reconstruction accuracy in spectral dimensionality reduction. Founded on the error source analysis of PCA from a geometric point of view, an objective function minimizing the within-cluster spectral reconstruction error is established to divide the error space of PCA. PCA is implemented again to each divided cluster to reduce the dimensionality of spectral reflectance. The proposed method, error-space-divided PCA (ESDPCA), is tested using four different spectral datasets. The root mean squared error (RMSE) and CIEDE2000 colour difference are adopted as the spectral and colorimetric evaluation metric respectively. Statistical results indicate that ESDPCA can outperform PCA by at least one principal component (PC) in colorimetric accuracy, while it can outperform PCA by at least two or three PCs in spectral accuracy. Comparisons with other three representative methods (i.e., LabPQR, LabRGB, and XYZLMS) show that ESDPCA outperforms them both in spectral and colorimetric accuracy significantly. In addition, the proposed method is robust for spectral datasets and compatible with few other methods involving PCA. Moreover, the computation complexity of ESPCA has the same order of magnitude as that of PCA.* © *2022 Society for Imaging Science and Technology.*
[DOI: 10.2352/J.ImagingSci.Technol.2022.66.2.020410]

1. INTRODUCTION

Visible spectral reflectance is the intrinsic physical property of materials and can be applied to characterize colour without metamerism phenomenon. This property has drawn considerable attention in the fields of high-fidelity colour reproduction [1, 2], fine art conservation [3, 4] as well as digital image archives [5, 6], especially with the diversity of light sources, the complexity of colour rendering devices, and also the increasing requirements of colour reproduction accuracy in recent years.

The major issue is that unlike the traditional trichromatic system, the spectral data, usually described by several dozens of dimensions, has become a tough challenge for data storage and communication between different rendering devices. It is necessary to reduce the dimensionality of the spectral data and to construct a lower-dimensional space for smooth data storage and communication. Here the low-dimensional space needs to satisfy the constraint that the space has the lowest possible dimensionality; besides, the spectral reflectance reconstructed from the space is as similar as possible to the original spectral reflectance.

Many methods, such as PCA [7–9], nonnegative matrix factorization [10], weighted canonical correlation regression [11], independent component analysis [12], XYZLMS [13], LabPQR [14], LabAB [15], LabRGB [16] and LabLab [17], have been proposed to reduce the dimensionality of the high-dimensional spectral reflectance. Among them, PCA method is extensively used for dimensionality reduction of spectral reflectance. This method reformulates the spectral reflectance as the weighted sum of a small number of orthogonal basis to remove the high correlations between different dimensions of the original spectral reflectance. It can achieve optimal spectral accuracy as it minimizes the RMSE between the original and the reconstructed spectral reflectance. However, the best spectral accuracy does not always mean the best colorimetric accuracy since the spectral sensitivity of human visual system is not a constant function of the spectral wavelengths. In other words, different wavelengths have different contributions to the perceived colour.

Recent studies have realized the situation and treated each wavelength differently according to their relative contributions to the perceived colour. Thus, many weighting functions with respect to luminous efficiency function, colour matching functions and human cone spectral sensitivities have been proposed to weight the spectral reflectance before the implementation of PCA [18–22]. These methods are regarded as weighted PCA. Due to the complexity of the mechanism of colour perception, most of these weighting functions are obtained by a trial and error technique. The relevant psychophysical experiment or a mathematical proof to find the optimal weighting function is still elusive. These methods have improved the colorimetric accuracy of the reconstructed spectral reflectance to some extent. However,

Received June 28, 2021; accepted for publication Oct. 24, 2021; published online Nov. 17, 2021. Associate Editor: Li Yang.
1062-3701/2022/66(2)/020410/7/$25.00

the improvement of the colorimetric accuracy usually comes at the sacrifice of the spectral accuracy. This compromise violates the original intention of spectral colour reproduction that reach the consistent reproduction of spectral reflectance, which will inevitably evoke metamerism phenomenon again. The main reason resulting in this dilemma is that these methods regard PCA only as a useful tool and focus chiefly on the weighted pre-processing of the original spectral reflectance while they pay little attention to the tool itself, which puts the cart before the horse.

Though the relationship between the spectral accuracy and the colorimetric accuracy is not strictly positively correlated, the colorimetric accuracy will be increased if the spectral error is smaller enough. In the limit, the colorimetric error will be zero if the spectral error is zero. The spectral error is the root cause of colorimetric error. To improve the colorimetric accuracy, the spectral accuracy should be improved first. This conforms to the original intention of spectral colour reproduction. Based on this point of view, PCA is selected in this study to investigate the feasibility of further improving the spectral accuracy and the colorimetric accuracy simultaneously since it already has the best spectral reconstruction accuracy compared with other methods.

The basic principle of PCA is reviewed and the source that leads to the error in spectral reconstruction is analysed from a geometric viewpoint. The control strategy and corresponding objective function that minimizes the spectral error is proposed to divide the error space of PCA. Then PCA is implemented again to each divided spectral cluster for dimensionality reduction. The influence of cluster number and PC number on the spectral and colorimetric accuracy is tested. The proposed method is also compared with other three representative methods to verify its effectiveness.

2. METHODS AND MATERIALS

2.1 *Principal Component Analysis*

A set of spectral reflectance vectors $\mathbf{r}_i \in \mathbf{R}^n (i = 1, 2, K, m)$ can be represented by $\mathbf{r}_i = \sum_{j=1}^{n} a_j \mathbf{v}_j$ and $\mathbf{v}_j$ are basis vectors. The objective of PCA is to find the orthonormal basis for the subspace $\mathbf{R}^l$ of $\mathbf{R}^n$ that minimizes

$$\min_{\mathbf{v}_j} \sum_{i=1}^{m} \|\mathbf{r}_i - \hat{\mathbf{r}}_i\|^2, \quad j = 1, 2, \ldots, l \le n \tag{1}$$

here $\hat{\mathbf{r}}_i = \sum_{j=1}^{l} a_j \mathbf{v}_j$ represent the approximated spectral reflectance. In practice, the dataset is usually mean-centred first $\boldsymbol{X} = [\mathbf{r}_1 - \bar{\mathbf{r}}\ \mathbf{r}_2 - \bar{\mathbf{r}} \ldots \mathbf{r}_m - \bar{\mathbf{r}}]$, where $\bar{\mathbf{r}} = 1/m \sum_{i=1}^{m} \mathbf{r}_i$ denotes the mean of the dataset. The minimums are the eigenvalues of matrix $\boldsymbol{X}\boldsymbol{X}^T$ arranged in the descending order and the solutions are the eigenvectors $\mathbf{u}_1, \mathbf{u}_2, \ldots, \mathbf{u}_n$ arranged corresponding to the eigenvalues. Then spectral reflectance of the dataset can be approximately reconstructed by

$$\hat{\mathbf{r}}_i = \bar{\mathbf{r}} + \sum_{j=1}^{l} b_j \mathbf{u}_j, \tag{2}$$

where b_j are called factor scores and can be interpreted geometrically as the projections of mean-centred $\mathbf{r}_i$ onto the basis vectors.

2.2 *Error Source Analysis*

When approximating the spectral reflectance in $\mathbf{R}^l$, the reconstruction error occurs due to abandoning of the orthogonal complement space of $\mathbf{R}^l$. Defining the orthonormal basis matrix of the orthogonal complement space as $\mathbf{U}^T = \{\mathbf{u}_{l+1}\ \mathbf{u}_{l+2}\ \ldots\ \mathbf{u}_n\}$, then the spectral error Δe_i can be calculated by:

$$\begin{aligned} \|\Delta e_i\|^2 = \|\mathbf{r}_i - \hat{\mathbf{r}}_i\|^2 &= \left\| \bar{\mathbf{r}} + \sum_{j=1}^{n} b_j \mathbf{u}_j - \bar{\mathbf{r}} - \sum_{j=1}^{l} b_j \mathbf{u}_j \right\|^2 \\ &= \left\| \sum_{j=l+1}^{n} b_j \mathbf{u}_j \right\|^2 = \left\| \mathbf{U}^{\perp} \mathbf{b}_i^{\perp} \right\|^2 = \sum_{j=l+1}^{n} b_j^2 \end{aligned} \tag{3}$$

here $\mathbf{b}_i^{\perp}$ are vectors for the spectral reflectance $\mathbf{r}_i$ in the orthogonal complement space.

An example of reducing a two-dimensional random dataset into one dimension is showed in Figure 1(a) from the intuitive geometric viewpoint. The dataset is obtained by generating evenly distributed random numbers between 0 and 2 first, and then selecting the numbers between line $y - x > -1$ and line $y - x < 1$. The blue solid arrow represents the first PC that the random dataset is reduced to, while the red dashed arrow represents the abandoned second PC. Then the reconstruction error for each sample is the length of the red dashed arrow which is parallel to the second PC. It is the distance of the sample point to the first PC. The total reconstruction error for the two-dimensional random dataset is the length accumulation of all the red dashed arrows.

2.3 *The Proposed Method*

The reconstruction error produced in PCA is the distance from the sample to $\mathbf{R}^l$ in $\mathbf{R}^n$ along the abandoned orthogonal complement space of $\mathbf{R}^l$. To decrease this error is to decrease the distance, namely to decrease the length of the red dashed arrows in Fig. 1(a). If several other lines parallel to the first PC are properly added to divide the dataset along the second PC and the smallest distance from the sample to the lines is taken as the new reconstruction error, as shown in Fig. 1(b), the length of most red dashed arrows will be cut short. In Fig. 1(b), the green thick arrow represents the first PC of Cluster 1 while the green thin arrows represent the reconstruction error for each sample of Cluster 1. The blue and red arrows represent the first PC and reconstruction error of Cluster 2 and Cluster 3, respectively. Obviously, the total error accumulation of the new red dashed arrows in Fig. 1(b) will be reduced significantly compared with that of the old red dashed arrows in Fig. 1(a). It indicates that by dividing the error space of PCA, the total reconstruction error can be decreased

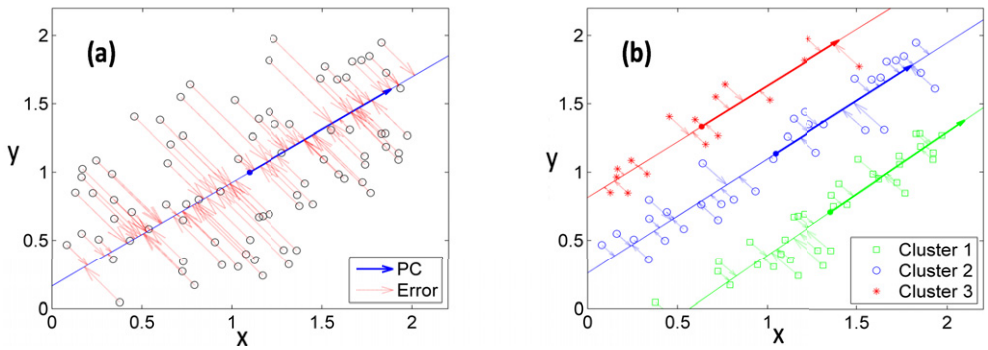

Figure 1. Schematic diagram of the proposed ESDPCA. (a) Error analysis of PCA in reducing a two-dimensional random dataset into one dimension. (b) Division of the abandoned second PC.

under the same reduced dimensionality, which satisfies the constraint required for spectral dimensionality reduction.

Similarly, for the high-dimensional spectral dataset, the total reconstruction error can be reduced by properly dividing the abandoned high-dimensional orthogonal complement space. If the spectral dataset $\mathbf{R}$ is divided into K clusters $\mathbf{R} = \{\mathbf{R}_1 \quad \mathbf{R}_2 \quad \dots \quad \mathbf{R}_K\}$ in the abandoned orthogonal complement space, to minimize the within-cluster reconstruction error, the objective function used for the division can be defined as follows:

$$\min \sum_{j=1}^{K} \sum_{\mathbf{r}_i \in \mathbf{R}_j} \|\mathbf{b}_i^{\perp} - \mathbf{c}_j\|^2, \tag{4}$$

where $\mathbf{c}_j$ is the mean of all the spectral reflectance in cluster $\mathbf{R}_j$. It is notable that the proposed method is equivalent to the original PCA when K equals 1. In this study, the K-means algorithm is applied to solve Eq. (4) by randomly selecting K factor score means for the m samples in the orthogonal complement space [23]. Due to the limited sizes of the spectral dataset, PCA is implemented again to each divided cluster for further reduction of the reconstruction error. Based on this principle, the proposed method is called error-space-divided PCA (ESDPCA).

2.4 *Materials*

Four spectral datasets, the Matt Munsell Atlas [24], the Natural Colour System (NCS) [25], a printing dataset and a mineral pigment dataset, are selected as the testing samples to investigate the proposed ESDPCA. The spectral reflectance of 1269 matt Munsell colour chips were measured at 1 nm wavelength interval between 380 and 800 nm by the Perkin-Elmer lambda 9 UV/VIS/NIR spectrophotometer; the spectral reflectance of 1675 colour chips from the NCS Atlas were measured at 10 nm intervals between 400 and 700 nm by the HunterLab UltraScan spectrocolourimeter; the 1473 colour chips of the printing dataset were printed by the Canon IPF5100 printer using the CMY inks and their spectral reflectance were measured by X-Rite Spectroscan at 10 nm intervals between 400 and 700 nm; the 1694 spectral reflectance of the mineral pigment dataset were measured by the GretagMacbeth SpectroEye^{TM} at 10 nm intervals between 400 and 700 nm. Here the spectral reflectance from the Matt Munsell Atlas was resampled at 10 nm intervals between 400 and 700 nm.

3. RESULTS AND DISCUSSIONS

3.1 *Analysis of ESDPCA*

Spectral reflectance from the Matt Munsell Atlas is selected as the testing sample to investigate the characteristics of ESDPCA. The spectral reflectance is firstly reduced into different dimensionalities (1–9) with different cluster numbers (1, 5, 10, 16 and 23). The spectral reflectance is subsequently reconstructed by linearly combining the orthogonal basis that spans the low-dimensional spaces. The RMSE between the original spectral reflectance and the reconstructed spectral reflectance is calculated as the metric of spectral accuracy. The CIE 2000 colour difference under the CIE 1931 standard observer and the CIE standard illuminant D65 is calculated to evaluate the colorimetric accuracy. Statistical results of RMSE and colour difference between the original spectral reflectance and the reconstructed spectral reflectance are shown in Tables I and II respectively.

Firstly, the performance of the proposed ESDPCA and the original PCA (the column titled '1 Cluster') is compared. It is obvious that the proposed method has a better performance both in spectral accuracy and colorimetric accuracy. ESDPCA can outperform PCA by at least one PC in colour difference, while it can outperform PCA by at least two or three PCs in RMSE. For example, the colour difference of ESDPCA with 23 clusters and 4 PCs is better than that of PCA with 6 PCs, while the RMSE of ESDPCA with 23 clusters and 4 PCs is significantly better than that of PCA with 8 PCs and comparable to that of PCA with 9 PCs. In other words, ESDPCA with 23 clusters and 4 PCs outperforms PCA by 4 PCs in RMSE, and 2 PCs in colour difference. This indicates that ESDPCA can reduce the dimensionality of the spectral reflectance significantly under the same accuracy constraint, which can facilitate the description and mapping of spectral colour gamut. The different performance of ESDPCA in spectral accuracy and colorimetric accuracy result from the nonlinear relationship between the spectral RMSE and colour difference. However, the colorimetric accuracy is

Table I. RMSE of ESDPCA with different PC and cluster numbers.

Number of PCs	1 Cluster (Original PCA)		5 Clusters		10 Clusters		16 Clusters		23 Clusters	
	Max	Mean	Max	Mean	Max	Mean	Max	Mean	Max	Mean
1	0.2571	0.0769	0.1323	0.0436	0.1043	0.0327	0.0913	0.0271	0.0702	0.0232
2	0.1638	0.0417	0.0725	0.0192	0.0713	0.0153	0.0449	0.0124	0.0415	0.0109
3	0.1060	0.0192	0.0444	0.0109	0.0266	0.0083	0.0234	0.0070	0.0240	0.0061
4	0.0744	0.0130	0.0271	0.0078	0.0172	0.0058	0.0146	0.0049	0.0129	0.0042
5	0.0550	0.0094	0.0220	0.0056	0.0167	0.0045	0.0128	0.0037	0.0097	0.0032
6	0.0303	0.0076	0.0159	0.0045	0.0133	0.0036	0.0106	0.0030	0.0096	0.0026
7	0.0302	0.0055	0.0122	0.0035	0.0080	0.0027	0.0067	0.0023	0.0057	0.0020
8	0.0172	0.0045	0.0086	0.0027	0.0064	0.0022	0.0050	0.0018	0.0042	0.0016
9	0.0146	0.0032	0.0061	0.0020	0.0051	0.0017	0.0047	0.0015	0.0036	0.0013

improved in ESDPCA on the basis of improving the spectral accuracy. Moreover, the colorimetric accuracy of ESDPCA can be further improved by the weighted processing of the original spectral reflectance since it already has excellent spectral accuracy and is compatible with weighted PCA.

Secondly, the advantage of error space division to the maximum spectral error is investigated. In terms of PCA, the spectral samples with a relatively decentralized distribution can lead to a large spectral reconstruction error, especially the maximum error. It is notable that the introduction of ESDPCA can reduce the maximum error remarkably. As shown in Table I, ESDPCA with 16 clusters and 2 PCs outperforms PCA with 4 PCs in mean RMSE, whereas it outperforms PCA with 5 PCs in maximum RMSE. Figure 2 illustrates the implementation of ESDPCA with 2 PCs and 5 clusters to the Matt Munsell Atlas spectral dataset from a geometric point of view. The length of the short black arrow is the maximum spectral error of ESDPCA along the abandoned third PC, while the length of the long black arrow is the maximum spectral error of PCA along the abandoned third PC. It is apparent that the maximum spectral error of ESDPCA is remarkably smaller than that of PCA.

Thirdly, the influence of cluster number and PC number on spectral reconstruction accuracy is considered. Tables I and II show that the reconstruction accuracy of spectral reflectance increases with the increasing of cluster number. For instance, the RMSE of ESDPCA with 4 PCs and 23 clusters is better than that of ESDPCA with 4 PCs and 5 clusters. In addition, with the same cluster number ESDPCA improves the reconstruction accuracy more and more as the number of PCs increases. For instance, the RMSE of ESDPCA with 23 clusters and 3 PCs is less than that of PCA with 6 PCs, whereas the RMSE of ESDPCA with 23 clusters and 4 PCs is less than that of PCA with 8 PCs.

Fourthly, the PCs of different clusters are compared to investigate their characteristics. ESDPCA with 6 PCs and 10 clusters is implemented on the Matt Munsell Atlas spectral dataset. The first 6 PCs of the 10 clusters are shown in Figure 3. It is apparent that, from the first PCs to the sixth PCs, the discrepancy between the PCs increases. This phenomenon can be attributed to the limited number of the spectral reflectance used for dimensionality reduction. As shown in Fig. 2, the discrepancy between the clusters in Fig. 2(b) is more scattered than that in Fig. 2(a), especially for the outmost clusters along the third PC. Thus, ESDPCA carries out PCA again to each divided cluster in order to improve the spectral reconstruction accuracy.

Finally, the computation complexity of ESPCA has the same order of magnitude as that of PCA. The computation complexity of PCA is $O(n^3 + n^2m)$ and K-means algorithm is $O(KIm(n-l)^{\frac{1}{\alpha}})$, where I is the number of iterations and α is a number greater than 1, relating to the computation complexity of Euclidean distance. According to the computation process, the complexity of ESDPCA is $O(n^3(K+1) + 2n^2m + KIm(n-l)^{\frac{1}{\alpha}})$. Since I and K are regarded as constants and $\alpha > 1$, the complexity of ESDPCA can be determined as $O(n^3 + n^2m)$. It has the same complexity classes as PCA.

3.2 *Comparison with Three Other Representative Methods*

In order to further evaluate the effectiveness of the proposed method, the performance of ESDPCA is compared with the three other representative methods, LabPQR, LabRGB, and XYZLMS. Four spectral datasets are selected as the testing samples. These four methods are implemented on each spectral dataset, and then converted back to reconstruct the spectral reflectance by applying the parameters describing the low-dimensional spaces. The RMSE between the original and the reconstructed spectral reflectance is calculated as the metric of spectral accuracy. The CIEDE2000 color difference formula was selected as the colorimetric metric. The colorimetric values for the color difference formula were calculated under the CIE 1931 standard observer and eleven illuminants. The illuminants are the CIE standard illuminants A, D50, D65, D90, F2, F7, F11, and four other actual LED light sources (Cooper DL11, GE Par30, Osram Diachroic, Solux Diachroic) [26]. The error space of ESDPCA is divided into 24 clusters and the dimensionality is reduced to 6 which is equal to that of LabPQR, LabRGB, and XYZLMS. Results of these four methods are shown in Tables III and IV respectively.

Table II. Colour difference of ESDPCA with different PC and cluster numbers.

Number of PCs	1 Cluster (Original PCA)		5 Clusters		10 Clusters		16 Clusters		23 Clusters	
	Max	Mean	Max	Mean	Max	Mean	Max	Mean	Max	Mean
1	31.724	16.176	28.916	10.765	23.072	7.897	18.815	6.388	17.532	5.372
2	45.741	12.008	21.013	4.460	13.739	3.401	10.742	2.561	10.612	2.402
3	12.886	2.173	10.343	1.099	6.074	0.861	5.446	0.742	5.331	0.649
4	9.336	1.221	4.978	0.677	4.610	0.557	3.135	0.453	2.797	0.402
5	2.900	0.557	1.939	0.310	1.572	0.268	1.066	0.194	1.295	0.186
6	2.915	0.554	1.181	0.222	1.208	0.195	0.956	0.180	0.836	0.146
7	2.286	0.116	0.780	0.089	0.570	0.074	0.699	0.069	0.430	0.059
8	0.920	0.095	0.671	0.066	0.387	0.058	0.353	0.049	0.322	0.048
9	0.937	0.087	0.334	0.053	0.320	0.048	0.269	0.040	0.211	0.036

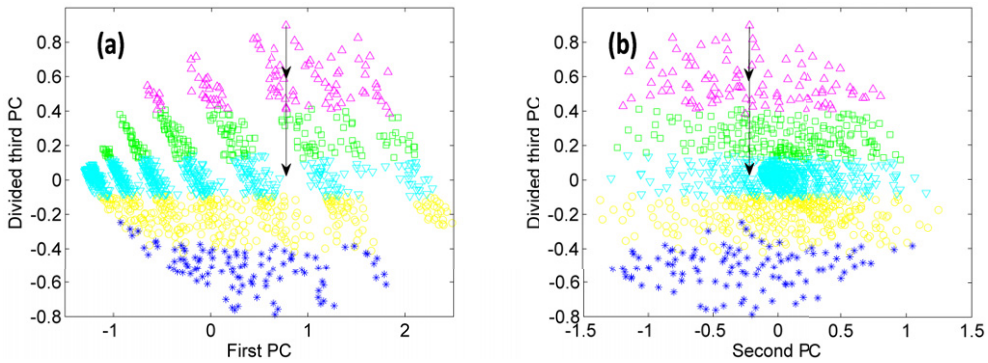

Figure 2. Implementation of ESDPCA on Matt Munsell Atlas spectral dataset with 2 PCs and 5 clusters. (a) The first PC and divided third PC, (b) the second PC and divided third PC.

Table III. RMSE of the four methods.

Samples	XYZLMS		LabRGB		LabPQR		ESDPCA	
	Max	Mean	Max	Mean	Max	Mean	Max	Mean
Matt Munsell Atlas	0.0569	0.0095	0.0590	0.0136	0.0558	0.0088	0.0075	0.0026
NCS	0.0685	0.0102	0.0665	0.0144	0.0635	0.0103	0.0123	0.0041
Printed Colour	0.0602	0.0159	0.0967	0.0347	0.0345	0.0114	0.0074	0.0009
Mineral Paint	0.0771	0.0160	0.0491	0.0123	0.0703	0.0142	0.0121	0.0022

It is obvious that XYZLMS, LabRGB and LabPQR have similar performances as their performances are inconsistent with the variation of the spectral datasets, while the performance of ESDPCA is remarkably better than them both in spectral accuracy and colorimetric accuracy for all the spectral datasets. It can be inferred that the performances of XYZLMS, LabRGB and LabPQR depend heavily on spectral datasets, whereas ESDPCA is relatively robust to spectral datasets. It is not difficult to conclude that ESDPCA has excellent capability in spectral dimensionality reduction for spectral colour reproduction.

4. CONCLUSIONS

A new method constructed by dividing the error space of principal component analysis (PCA) is proposed to reduce the spectral dimensionality for spectral colour reproduction. It improves colorimetric accuracy at the foundation of improving spectral accuracy in spectral reconstruction, which conforms to the original intention of spectral colour reproduction. Comparisons with traditional PCA suggest that the colorimetric accuracy of ESDPCA is better than that of PCA by at least one PC, while ESDPCA can outperform PCA by at least two or three PCs in RMSE. With the same PC numbers, the performance of ESDPCA becomes better with the increase of division number, and with the same

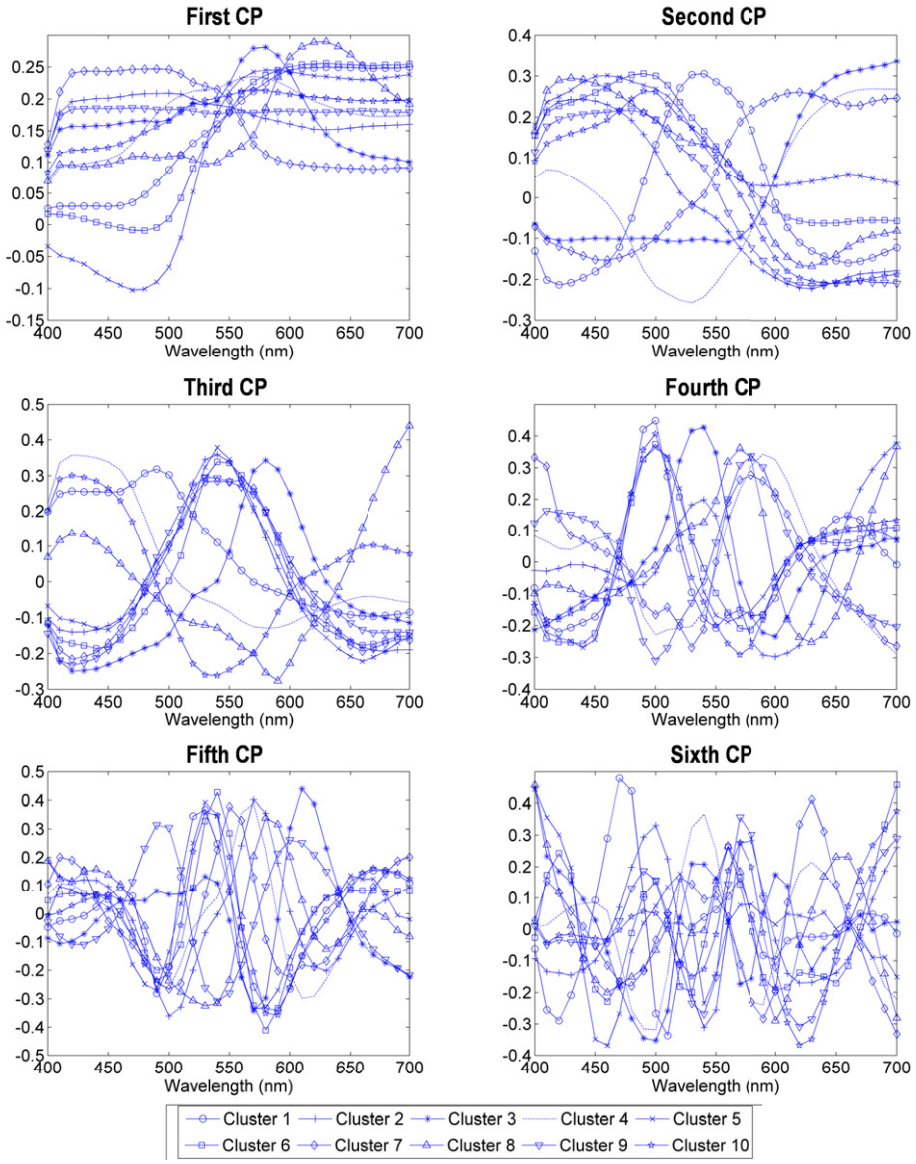

Figure 3. The first six PC vectors of ten clusters.

Table IV. Colour difference of the four methods.

Samples	XYZLMS		LabRGB		LabPQR		ESDPCA	
	Max	Mean	Max	Mean	Max	Mean	Max	Mean
Matt Munsell Atlas	2.755	0.228	1.186	0.313	2.822	0.208	0.777	0.160
NCS	2.195	0.215	1.377	0.303	2.403	0.204	0.807	0.163
Printed Colour	1.622	0.459	2.041	1.161	0.730	0.307	0.459	0.081
Mineral Paint	3.227	0.258	1.398	0.284	4.615	0.520	1.144	0.141

division number the performance of ESDPCA is better and better as the PC number increases. Comparisons with three representative methods indicate that the proposed ESDPCA can outperform them remarkably both in spectral accuracy and colorimetric accuracy for all the spectral datasets and it is also robust to spectral datasets. Besides, ESDPCA can be extended to LabPQR to further improve its accuracy since the PQR components of LabPQR are also derived by PCA. Due to its excellent compatibility, ESDPCA can also be combined with weighted PCA. All these imply that the proposed method will deliver better performance in spectral colour reproduction.

ACKNOWLEDGMENT

This work was supported by the National Natural Science Foundation of China (grant number 61575147); the Key Scientific and Technological Project of Henan Province under (grant number 192102310028); the General Project for Humanities and Social Sciences Research of the Education Department of Henan Province Key laboratory fund (grant number 2019-ZZJH-128), Lab of Green Platemaking and Standardization for Flexographic Printing (No. ZBKT201905) and the Science and Technology Innovation Team of Henan University of Animal Husbandry and Economy.

REFERENCES

[1] Y. Wang, S. Zhai, and Z. Wang, "Multispectral image reproduction via color appearance mapping," Int. J. Signal Process. Image Process. Pattern Recognit. **7**, 65–72 (2014).

[2] N. Ansari, O. Alizadeh-Mousavi, H.-P. Seidel, and V. Babaei, "Mixed integer ink selection for spectral reproduction," ACM Trans. Graph. **39**, 1–16 (2020).

[3] J. Striova, A. Dal Fovo, and R. Fontana, "Reflectance imaging spectroscopy in heritage science," Riv. Nuovo Cimento **43**, 515–566 (2020).

[4] I. El-Rifai, H. Mahgoub, and A. Ide-Ektessabi, "Multi-spectral imaging system (IWN) for the digitization and investigation of cultural heritage," *Euro Mediterr. Conf.* (Springer, Cham, 2016), pp. 232–240.

[5] N. Tanaka and K. Mochizuki, "A digital archive method based on multispectral imaging with goniometric multiband camera," Bull. Japan Soc. Sci. Des. **61**, 335–344 (2014).

[6] N. Benedict, "Digital Approaches to the Archive: Multispectral Imaging and the Recovery of Borges's Writing Process in 'El muerto' and 'La casa de Asterión'," Variaciones Borges **45**, 153–170 (2018).

[7] H. S. Fairman and M. H. Brill, "The principal components of reflectances," Color Res. Appl. **29**, 104–110 (2004).

[8] D. Y. Tzeng and R. S. Berns, "A review of principal component analysis and its applications to color technology," Color Res. Appl. **30**, 84–98 (2005).

[9] X. Zhang and H. Xu, "Reconstructing spectral reflectance by dividing spectral space and extending the principal components in principal component analysis," J. Opt. Soc. Am. A **25**, 371–378 (2008).

[10] V. P. Pauca, J. Piper, and R. J. Plemmons, "Nonnegative matrix factorization for spectral data analysis," Linear Algebr. Appl. **416**, 29–47 (2006).

[11] N. Eslahi, S. H. Amirshahi, and F. Agahian, "Recovery of spectral data using weighted canonical correlation regression," Opt. Rev. **16**, 296–303 (2009).

[12] J. Wang and C.-I. Chang, "Independent component analysis-based dimensionality reduction with applications in hyperspectral image analysis," IEEE Trans. Geosci. Remote Sens. **44**, 1586–1600 (2006).

[13] X. Zhang, Q. Wang, Y. Wang, and H. Wu, "XYZLMS interim connection space for spectral image compression and reproduction," Opt. Lett. **37**, 5097–5099 (2012).

[14] S. Tsutsumi, M. Rosen, and R. Berns, "Spectral gamut mapping using LabPQR," J. Imaging Sci. Technol. **51**, 473–485 (2007).

[15] S. Le Moan and P. Urban, "A new connection space for low-dimensional spectral color management," Proc. SPIE **9018**, 90180E (2014).

[16] F. Nakaya and N. Ohta, "Applying LabRGB to real multi-spectral images," *Proc. IS&T/SID CIC16: Sixteenth Color Imaging Conf.* (IS&T, Springfield, 2008), pp. 289–294.

[17] Q. Cao, X. Wan, J. Li, and J. Liang, "Updated version of an interim connection space LabPQR for spectral color reproduction: LabLab," J. Opt. Soc. Am. A **33**, 1860–1871 (2016).

[18] Q. Cao, X. Wan, J. Li, Q. Liu, J. Liang, and C. Li, "Spectral data compression using weighted principal component analysis with consideration of human visual system and light sources," Opt. Rev. **23**, 753–764 (2016).

[19] J. Tian and Y. Tang, "Wavelength-sensitive-function controlled reflectance reconstruction," Opt. Lett. **38**, 2818–2820 (2013).

[20] G. Wu, Z. Liu, E. Fang, and H. Yu, "Reconstruction of spectral color information using weighted principal component analysis," Optik **126**, 1249–1253 (2015).

[21] G. Wu, X. Shen, Z. Liu, and J. Zhang, "Wavelength-sensitive-function-based spectral reconstruction using segmented principal component analysis," Opt. Appl. **46** (2016).

[22] G. Wu, L. Qian, G. Hu, and X. Li, "Spectral Reflectance Recovery from Tristimulus Values under Multi-Illuminants," J. Spectrosc. **2019** (2019).

[23] M. Ahmed, R. Seraj, and S. M. S. Islam, "The k-means algorithm: A comprehensive survey and performance evaluation," Electronics **9**, 1295 (2020).

[24] Munsell colors matt (Spectrofotometer measured) [Internet]. Eastern Finland: University Of Eastern Finland, Spectral Color Research Group. [cited 2020]. Available from: http://www.uef.fi/web/spectral/databases-and-software.

[25] F. Ayala, J. F. Echávarri, P. Renet, and A. I. Negueruela, "Use of three tristimulus values from surface reflectance spectra to calculate the principal components for reconstructing these spectra by using only three eigenvectors," J. Opt. Soc. Am. A **23**, 2020–2026 (2006).

[26] National Gallery: Spectral Power Distribution (SPD) Curves [Internet]. London: Joseph Padfield. [cited 2020]. Available from: http://research.ng-london.org.uk/scientific/spd/.